partially stabilized zirconia phases (Evans & Cannon, 1986). In superconductors, local changes in structure may lead to unfavorable copper–oxygen configurations which can have strong effects on the critical current, because its magnitude is determined by the critical current of the grain boundaries and their strained surroundings.

At present there are not enough data to quantify the occurrence and the magnitude of strain, and thus direct correlation with the critical current data is not possible. However, high-resolution electron microscopy shows that the strain is highly localized near the grain boundary (see Figs. 4 and 5). Research will be continued on these strain observations in both the orthorhombic and tetragonal forms.

In summary, we have found that dense polycrystalline $YBa_2Cu_3O_{7-\delta}$ materials prepared by sintering of pressed pellets without sintering aids develop random grain boundaries, but highly faceted along (001). There are no observed second phases, but sometimes highly localized strain fields at the grain boundaries. The structural discontinuities observed may very well explain the low critical currents obtainable in polycrystalline superconductors which have randomly oriented grains.

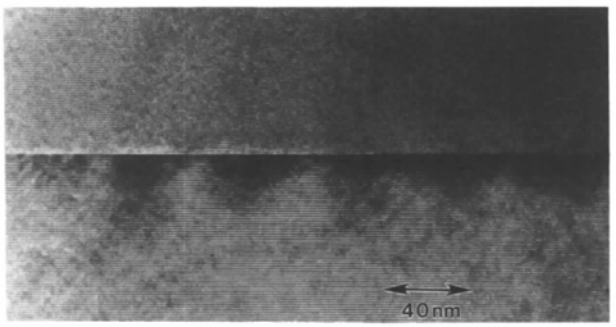

Fig. 5. Grain boundary of two grains approximately in [110] (top) and [100] (bottom) orientation. At each position where a unit cell of the top grain ends at the boundary, a strain center occurs in the bottom grain. This indicates that the upper grain grew to impingement on the lower grain.

The authors thank M. Y. Chu and Dr L. C. DeJonghe for providing the specimen. This work was supported by the Director, Office of Energy Research, Office of Basic Energy Sciences, Materials Science Division, US Department of Energy, under contract No. CE-AC03-76SF00098.

References

EVANS, A. G. & CANNON, R. M. (1986). *Mechanical Properties and Phase Transitions in Engineering Materials*, edited by S. D. ANTOLOVICH *et al.*, p. 409. New York: Metallurgical Society, AIME.

GRONSKY, R. & THOMAS, G. (1983). *Proc. 41st Annu. Meet. Electron Microsc. Soc. Am.*, edited by G. W. BAILEY, pp. 310–311. Baton Rouge: Claitor.

JIN, S., SHERWOOD, R. C., TIEFEL, T. H., VAN DOVER, R. B., FASTNACHT, R. A., NAKAHARA, S., YAN, M. F. & JOHNSON, D. W. (1987). Proc. Materials Research Society Fall Meet., Boston, 1987.

SAXTON, W. O. (1978). *Inst. Phys. Conf. Ser.* No. 44. London: Institute of Physics.

THOMAS, G. (1988). *Role of Interfaces.* Ceram. Microstruct. Conf. 1986. New York: Plenum.

ZANDBERGEN, H. W., GRONSKY, R., CHU, M. Y., DEJONGHE, L. C., HOLLAND, G. & STACY, A. M. (1987). Proc. Materials Research Society Fall Meet., Boston, 1987.

ZANDBERGEN, H. W., GRONSKY, R. & THOMAS, G. (1988). *Phys. Status Solidi.* In the press.

ZANDBERGEN, H. W., HETHERINGTON, C. J. D. & GRONSKY, R. (1988). Submitted to *J. Supercond.*

Acta Cryst. (1988). A**44**, 775–780

A Contribution to the Unsolved Problem of a High-Tilt Fully Eucentric Goniometer Stage

BY U. VALDRÈ

Dipartimento di Fisica, CISM and GNSM-CNR, Università di Bologna, Via Irnerio 46, 40126 *Bologna, Italy*

AND K. TSUNO

JEOL Ltd, 1418 *Nakagami, Akishima, Tokyo* 196, *Japan*

(*Received* 30 *November* 1987; *accepted* 17 *March* 1988)

Abstract

A design is presented of a high-angle fully eucentric tilting stage (±45, ±23° around two orthogonal axes) for a transmission electron microscope. The concurrent design of suitable objective-lens pole pieces has been made in order to get the best compromise between electron optical performances and the difficulties inherent in the construction of the stage. A resolution of 3 Å is calculated at an accelerating voltage of 200 kV. The design exploits the space both above and in the middle of the objective pole-piece

0108-7673/88/060775-06$03.00

assembly: the space above is used to house the stage, while the space in the lens gap serves the purpose of loading the specimen. In this way the incorporation of an x, y, z specimen traverse stage inside the high-tilt universal suspension appears to be a practical proposition. Although the details of the stage have been worked out with the JEOL JEM 100 and 2000 series of electron microscopes in mind, the working principles of the design can be applied to other types of microscopes.

Introduction

Tilting of the specimen in an electron microscope without producing level changes (along the optical z axis) and lateral shift (in the x, y traverse plane) of the observed area is the ideal requirement for the many diffraction-contrast experiments in which it is essential to set the orientation of the specimen with respect to the beam in a transmission electron microscope (TEM).

A tilting stage which fulfils this requirement is called a (full) eucentric stage. Only two stages of this type have been described so far [Leteurtre, as reported by Genty (1972); Valdrè (1975)] and only the former was built; they suffer, however, from low angles of tilt (8–15°) and low resolution, and require the replacement of the whole specimen chamber. The problem of a high-tilt fully eucentric stage has not yet been solved. The so-called eucentric stages commercially available are in fact only axially eucentric, *i.e.* there may be no shift and/or z changes of the specimen during tilting if this is performed around only one specific axis out of two orthogonal axes of tilt. The difficulty in solving the problem of eucentricity arises from the restricted space available in the objective pole-piece region and from the avoidance of any interference between tilt and traverse.

Since the continuing progress and expansion of electron microscopy of thin crystals demands ever more accurate high-angle and versatile specimen stages, a new attempt has been made to produce a satisfactory eucentric stage.

For a stage to be truly eucentric, the specimen traverse must be built inside the tilting mechanism, and the tilt axes should intersect at a point (centre of the gimbals) where the observed area must be placed. At present, the use of devices other than mechanical ones (*e.g.* piezoelectric, magnetic, thermal elements), which could ease the solution and reduce the mechanical complexity of the stage, does not seem feasible. This is still true even if great progress has recently been achieved in the use of piezoelectric elements, in connection with the development of the scanning tunneling microscope (STM) and of its incorporation in TEMs (Spence, 1988), because of the wide range of traverse values required in a TEM or in a scanning transmission electron microscope (STEM).

These facts leave two independent ways to tackle the problem: (i) the use of large-bore large-gap magnetic lenses of good performances for conventional operating voltages (100 kV) (usually better performances can be obtained at higher voltages owing to the scaled up size of the objective lens); and (ii) the exploitation of all the various possibilities offered by the geometry of the lenses and specimen region. In the following, advantage has been taken of both ways.

It should be noted that there is a conflict between the requirements of high-performance lenses and that of large space in the pole-piece region for housing a complex stage; usually lenses are designed for the highest possible resolution. In the present case priority was given to a geometry suitable for an overall stage feasibility, then the free parameters of the lens and the details of the stage design were both changed, in a sort of iterative process, in order to optimize the resolution and to improve the features of the eucentric stage. It was therefore necessary to assess, first of all, the effect on the resolution of the parameters controlling the performance of large gap and bore lenses.

For reasons of convenience (in particular, to have available a microscope for testing the 'to be constructed' stage), it was decided to design the eucentric tilting stage and the new lens geometry to fit the specimen chamber and the objective pole-piece casing respectively of the microscopes of the JEOL JEM 100 and 2000 series equipped with side entry ports.

Objective pole-piece design

Magnetic lenses with a large top bore (up to 20 mm) have been studied in the past (Yanaka & Watanabe, 1966), but their size is still not adequate for our purposes. In order to design an objective lens with the best electron optical performance consistent with the requirements of a eucentric stage, finite-element-method calculations (Munro, 1975; Tsuno & Smith, 1986) have been made, which take into account both the shape and size of very large pole pieces. The results are summarized below and refer to a lens whose geometrical parameters are indicated in Fig. 1 [preliminary results were reported by Valdrè & Tsuno (1986)].

Firstly, general relations between important pole-piece parameters (as indicated in Fig. 1) and the spherical aberration coefficient C_s are given.

Fig. 2 shows C_s *versus* $S+B_1$ (here $S=S_1+S_2$ is the gap length and B_1 the upper bore diameter of the lens) under the condition of a specimen located in the middle of the gap. The bold line shows C_s against S for B_1 extremely small (approaching zero). The thin lines show the effect of B_1 on C_s for various values of S. C_s increases linearly with both S and B_1; however, the effect on C_s of a fractional change $\mathrm{d}B_1/B_1$ is only about 10% of the effect of an equal change $\mathrm{d}S/S$.

Fig. 3 shows an example of the effect of specimen position Z_0 on C_s, C_c (the chromatic aberration coefficient) and f_0 (the focal length) for a lens with $S = 12$, $B_2 = 16$, $B_1 = 40$ and $D_2 = 48$ mm. Z_0 is measured from the bottom pole face. The increase in C_s by increasing Z_0 is significant. If the specimen could be located in the middle of the gap ($Z_0 = 6$ mm), C_s would have a value of only 2·6 mm, but if the specimen is set at $Z_0 = 10$ mm, C_s rapidly increases to 4·8 mm. Therefore, it must be concluded that the smaller B_1, S_2 and S are, the better the lens performance, *i.e.* the smaller the coefficients C_s and C_c (only C_s is shown in Fig. 2, but C_c shows the same variation).

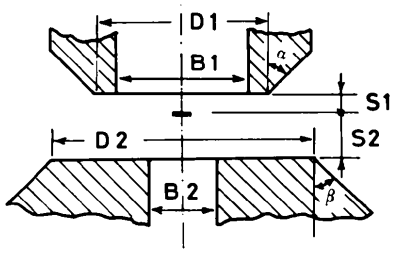

Fig. 1. The geometrical pole-piece parameters used in the text for describing the objective-lens pole pieces. The lens adopted has $B_1 = 40$, $B_2 = 16$, $D_1 = D_2 = 46$, $S = S_1 + S_2 = 12$, $S_1 = 2$ mm.

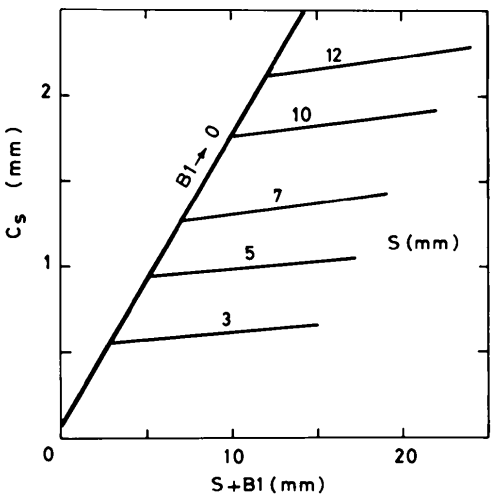

Fig. 2. Minimum values of C_s against gap S and upper pole-piece bore B_1. The specimen is assumed to be located in the middle of the lens gap.

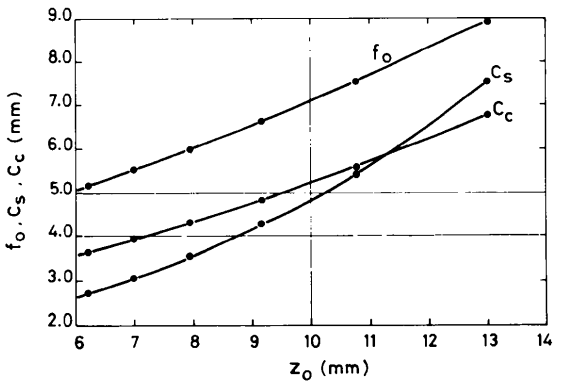

Fig. 3. Dependence of focal length f_0, C_s and C_c on the specimen position Z_0 for a lens having $B_1 = 40$, $B_2 = 16$, $S = 12$ and $D_2 = 48$ mm. Z_0 and f_0 are both measured from the bottom pole-piece face.

The conditions required by a fully eucentric stage having $B_1 = 40$, $S = 12$ and $S_2 = 10$ mm do not allow much latitude from the point of view of lens design. The only, although little effective, choice is to optimize the lens by varying the remaining parameters (D_1, D_2, B_2, α and β; see Fig. 1).

The most important factor is B_2. Fig. 4 shows the dependence of C_s, C_c and f_0 on B_2 for the chosen values of B_1, S and S_2. For each value of B_2, the optimum shape was selected to minimize C_s. C_s reaches a minimum value when B_2 is in the range 16–24 mm. C_c and f_0 increase monotonically with B_2.

As seen from Fig. 5, C_s decreases monotonically with increasing D_2 for every value of B_2. Thus, a flat-bottomed pole piece is recommended. The effect of D_2 is negligible above 40 mm, which is near to the maximum value allowed by the pole-piece assembly of the standard JEM 100 and 2000 series.

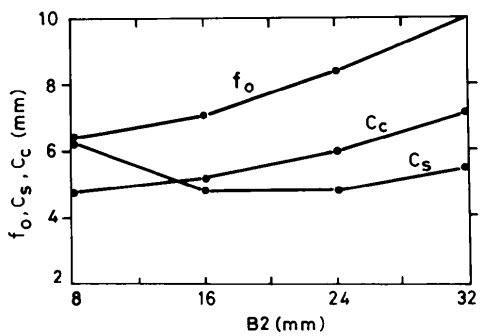

Fig. 4. f_0, C_c and C_s *versus* the bottom pole-piece bore B_2, for $B_1 = 40$, $S = 12$ and $S_1 = 2$ mm.

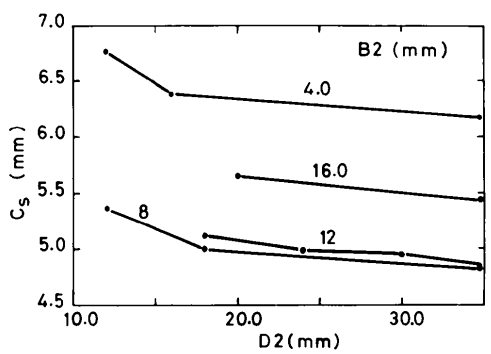

Fig. 5. C_s *versus* D_2 (the outer diameter of the flat face of the bottom pole piece), for various values of its bore B_2 (in mm).

In our special case where B_1 has to be large to accommodate the stage, the peak of the magnetic field distribution is close to the bottom pole face. In order to increase the optical performance it is desirable to place the specimen in the highest magnetic field position, while in order to achieve high tilting angles the specimen level should be high (4 mm above the mid-gap plane). It is therefore necessary to move the field peak towards the upper pole piece. Since, as a general rule, the field peak moves towards a sharp pole-piece face and a narrow bore side, D_1 should be small (though its effect is marginal), α should be small and β large. However, since B_1 is large, only α, β and D_1, D_2 can be adjusted to bring the field peak position towards the upper pole piece. Hence the top pole piece should have a sharp taper with a narrrow face and the bottom pole piece should be flat.

On the basis of these results an asymmetrical lens design was chosen with $B_2 = 16$ mm, D_2 equal to the outer diameter of the pole piece (with this choice β

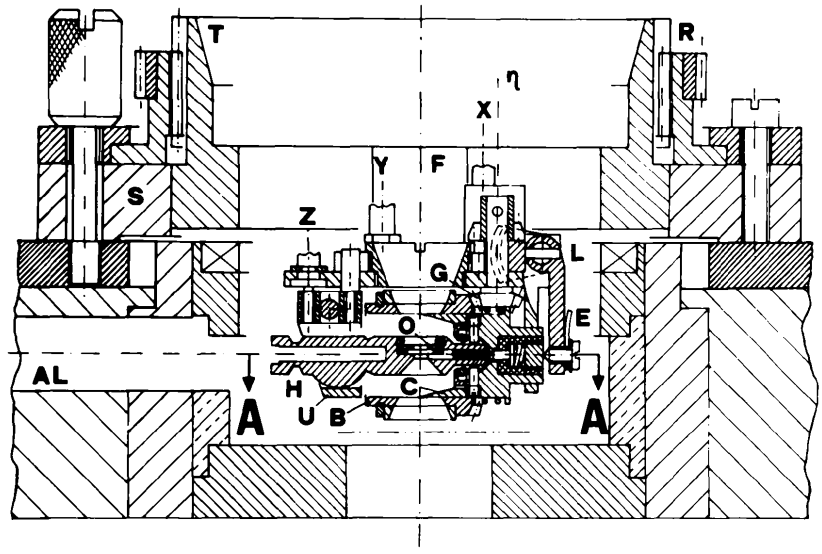

(a)

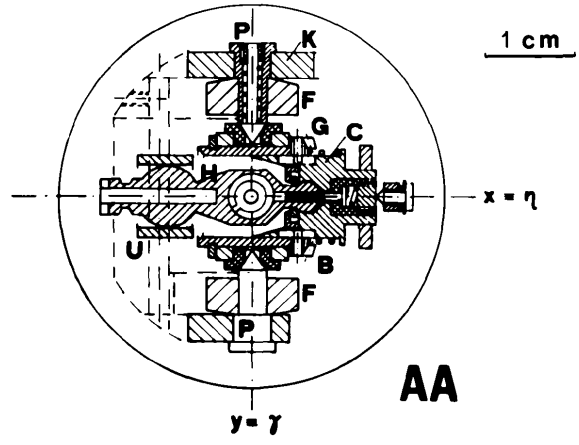

(b)

Fig. 6. To-scale cross-sectional drawing of the eucentric stage placed within the pole-piece region of the objective lens. (*a*) A section with a plane passing through the axis of the column of the electron microscope. (*b*) A section of (*a*) through *AA*. Note the eucentric stage is appended, *via* pins *P*, *P*, to legs *F*, *F* of the top lifting stage *T* which is bolted to the standard traverse stage *S* of the microscope. *H* is the specimen holder; it is loaded in the stage through side hole *AL* by means of a clamp and of a side-entry type of air lock. *X*, *Y*, *Z* indicate the shafts for controlling the three orthogonal movements of the specimen *O* within the tilt stage. *U*: fork activated by *Y* and *Z* for supplying the *y*, *z* traverses to the specimen. *G*: gear for rotating barrel *B*. *C*: carrier for the head of the specimen holder *H*. *L*: lever operated by *X* to provide the *x* traverse. *E*: electrical lead and contact to the specimen. η, γ: axes of tilt, coincident with the *x* and *y* traverses respectively.

is practically equal to 90°), $D_1 = 46$ mm (*cf.* $B_1 = 40$ mm) and $\alpha = 0°$. The lens would be run at low excitation (7000 A turns at 200 kV) and, for TEM, the electron optical features are $C_s = 4{\cdot}8$, $C_c = 5{\cdot}2$ mm and a long focal length, $f_0 = 7{\cdot}1$ mm. The estimated resolution (taking into account spherical and diffraction errors) is 3–5 Å in the 200–100 kV range; 2 Å resolution should be obtainable at higher voltages.

Double-tilt eucentric stage design

A eucentric stage to fit the above-mentioned lens has been designed. After examining various possible solutions, it appeared that the use of a top-driven stage combined with a side-entry specimen holder would be the most advantageous. Consequently, the main general features of the stage are: (i) the specimen *O* is mounted in a special holder *H* (Figs. 6 and 7), which is inserted in the tilting stage by means of a clamp-and-release rod mechanism (not shown in Fig. 6) *via* a side-entry air lock; (ii) the tilting-stage controllers operate the device from above the objective lens casing (*e.g.* *X*, *Y*, *Z*).

The specimen stage can be considered to be made up of three parts: the top lifting stage *T*, the tilting device (Fig. 6*b*) and the bottom traverse stage (incorporated in the tilt stage). The top lifting stage is mounted in the standard traverse stage *S* of the microscope and replaces the aluminium platform where the ordinary cartridge usually sits. In this way the overall stage has three degrees of freedom: the two

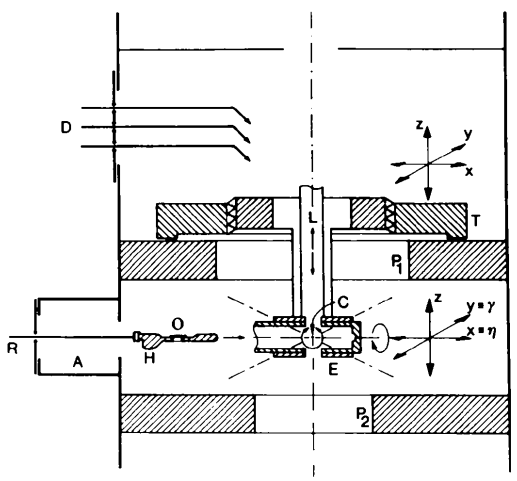

Fig. 7. Schematic representation of the proposed eucentric stage. *A*: air lock; *C*: intersection of the ±23° tilt (γ) axis with the foil plane; *D*: flange with drives for traverse and eucentric stages; *E*: eucentric stage incorporating *z* adjustment and *x*, *y* specimen traverse; *H*: specimen holder; *L*: leg incorporating a vertical adjustment device for setting the eucentricity (crossing of γ and η axes of tilt); *O*: specimen; *P*1, *P*2: pole pieces; *R*: rod with clamp for loading the specimen holder; *T*: top traverse stage with *x*, *y*, *z* adjustments; η: ±45° axis of tilt coincident with the direction of the *x* specimen traverse.

standard traverses and the (*z*) vertical motion. The *z* movement is obtained by rotating screw *R*. These three orthogonal movements are used for aligning the eucentric stage with respect to the optical axis and for setting its level in the lens gap. Once adjusted they should not be touched, except for re-setting if the stage, for some reason, has been removed from the microscope.

The eucentric stage is appended to two legs *F*, *F* machined in the top lifting stage *T* and is formed by pivots *P*, *P* (γ axis of tilt) and by a barrel *B*, whose axis of symmetry is the η axis of tilt. The barrel can rotate by means of conical gears *G* by any angle, even greater than 360°. Tilt around the γ axis is obtained by a lever (not visible in Fig. 6) acting on clamp *K*.

Inserted in and engaged with barrel *B* is hollow cylinder *C* which follows the rotation of the barrel. Cylinder *C* carries the specimen holder *H* and can also slide inside the barrel to provide the *x* traverse of the specimen. This motion is produced by a lever *L* operated by a sector gear and by controller *X*. Holder *H* is provided with a spherical head which can pivot in a conical recess machined in *C*; this allows the *y* traverse and the *z* adjustment (both through arcs) of the specimen. The spherical head is held by an elastic split ring. A groove-and-pin coupling is used to drag the holder when the barrel and the cylinder rotate. The *y* movement is obtained by a *U*-shaped support *U* acting on the tail of *H* and operated by controller *Y*. Raising or lowering *U* by means of *Z* produces the *z* adjustment. A leaf spring (not shown) holds *H* in contact with *U*. It should be noted that the *x* traverse axis coincides with the η tilt axis and that the (small) *y* traverse occurs practically along the γ axis of tilt.

The *x* and *y* traverses are both ±1·5 mm, the *z* adjustment is ±0·5 mm, the useful tilt angle around the η axis is ±45° (however, the specimen can be turned upside down) and the tilt angle around the γ axis is ±23°. A means (eucentricity controller) is also provided for adjusting the γ axis in order for it to intersect the η axis at a point (centre of the universal suspension).

Altogether nine controllers are needed for the various functions, four of which are for the initial setting operation (*x*, *y* standard traverse, level and eucentricity adjustments). Out of the remaining five controllers, one is for setting the specimen level inside the gimbals at each specimen change, if required; the other four controllers are the two couples of drives for the inner *x*, *y* traverses and for tilting. Interference between the various movements is avoided by gear-to-worm couplings; backlash is prevented by spring loading the controllers.

Provisions are made for collecting electric signals from the specimen *via* lead *E*, since the specimen may be electrically insulated (although usually

earthed). E is placed at the end of lever L and is elastically and electrically connected to the central part of the holder head.

The objective aperture and the decontaminator blade are placed below the straight broken line which has been drawn in Fig. 6(a) just above the bottom pole-piece face.

Both the standard specimen chamber and the basic x, y stage of the JEM 100 and 2000 series of microscopes are retained; the former is used for housing the additional drives needed to set and control the stage, and the latter for supporting the lifting and the tilting stages. A side-entry air lock is adopted for loading the specimen holder into the eucentric stage by means of a clamping jig, which is then withdrawn from the microscope.

Besides its application in tilting experiments, the stage will be useful in cases where both top and bottom surfaces of the specimen have to be investigated and, with little modification, for glancing-angle (reflection) microscopy (Cowley, 1988). In addition, provisions are made for the study of semiconductor devices by means of the electron beam induced current (EBIC) method, or for heating the sample. The present lens and stage features should also ease the incorporation of scanning tunneling facilities in a transmission electron microscope.

The development of the device is at a stage where detailed workshop drawings have been made and therefore its construction, even if complex, is feasible; it is however difficult to predict such uncertainties as mechanical instabilities. It is worthwhile to try to simplify further the mechanical solutions adopted, before proceeding to the construction of the eucentric tilting stage, in particular by attempting to incorporate piezoelectric elements in the design.

This research has been partly supported by Ministero Pubblica Istruzione, Rome.

References

COWLEY, J. M. (1988). *Reflection Electron Microscopy.* In *Surface and Interface Characterization by Electron Optical Methods*, edited by A. HOWIE & U. VALDRÈ. London: Plenum.

GENTY, B. (1972). In *Methodes et Techniques Nouvelles d'Observation en Métallurgie Physique*, p. 29. Paris: Societé Francaise de Microscopie Electronique.

MUNRO, E. (1975). A set of computer programs for calculating the properties of electron lenses. Rep. CUED/B-Elect TR45. Cambridge Univ. Engineering Department, Cambridge, England.

SPENCE, J. C. H. (1988). *Ultramicroscopy.* In the press.

TSUNO, K. & SMITH, K. C. A. (1986). XI*th Int. Congr. of Electron Microscopy, Kyoto*, 1986, Vol. I, pp. 295-296. Tokyo: Japanese Society of Electron Microscopy.

VALDRÈ, U. (1975). In *Electron Microscopy in Materials Science*, EUR 5515e, pp. 113-132. Luxembourg: Commission of the European Communities.

VALDRÈ, U. & TSUNO, K. (1986). XI*th Int. Congr. of Electron Microscopy, Kyoto*, 1986, Vol. II, pp. 925-926. Tokyo: Japanese Society of Electron Microscopy.

YANAKA, T. & WATANABE, M. (1966). VI*th Int. Congr. of Electron Microscopy, Kyoto*, 1966, Vol. I, pp. 141-142. Tokyo: Maruzen.

Acta Cryst. (1988). A**44**, 780-788

Results of Multislice Matrix Calculations for Convergent-Beam RHEED Patterns

BY ANDREW E. SMITH

Department of Physics, Monash University, Clayton, Victoria 3168, *Australia*

AND D. F. LYNCH

CSIRO, Division of Materials Science and Technology, Locked Bag 33, *Clayton, Victoria* 3168, *Australia*

(*Received* 30 *November* 1987; *accepted* 21 *March* 1988)

Abstract

Results of dynamical convergent-beam reflection high-energy electron diffraction (CBRHEED) calculations are presented for the (001) surface of magnesium oxide, the (111) surface of silicon and the (001) surface of molybdenum disulfide. These double rocking calculations are performed using a dynamical scattering approach. This is based on the evaluation of the surface parallel multislice matrix for the reflection (*i.e.* Bragg) geometry with account taken of the boundary conditions. Comparison with experimental results reported in the literature for these surfaces shows that only a full dynamical calculation with an appropriate number of beams is capable of a detailed description of the experimental contrast distributions. In particular, the nature of surface-wave-resonance effects is discussed.

1. Introduction

Though widely employed during the early years of electron diffraction (*e.g.* Finch, Quarrell & Wilman,

0108-7673/88/060780-09$03.00